

Better-Than-Chance Classification for Signal Detection

Jonathan Rosenblatt Roei Gilron Roy Mukamel

August 31, 2016

Abstract

We show that using a classifier’s accuracy as a test statistic, is underpowered for the purpose of finding a difference between populations, compared to a bona-fide statistical test. For the cases that the goal of the test is not the existence of a difference between populations, but the actual classification ability, we suggest several improvements to the classification accuracy, to increase its power against a “pure chance” null.

1 Introduction

A common workflow in neuroimaging consists of fitting a classifier, and estimating its predictive accuracy using cross validation. Given that the cross validated accuracy is a random quantity, it is then common to test if the cross validated accuracy is significantly better than chance using a permutation test. Examples in the neuroscientific literature include Golland and Fischl [2003], Pereira et al. [2009], Varoquaux et al. [2016], and especially the recently popularized *multivariate pattern analysis* (MVPA) framework of Kriegeskorte et al. [2006]. This practice is also observed in some high profile publications in the genetics literature: Golub et al. [1999], Slonim et al. [2000], Radmacher et al. [2002], Mukherjee et al. [2003], Juan and Iba [2004], Jiang et al. [2008].

To fix ideas, we will adhere to a concrete example. In Gilron et al. [2016], the authors seek to detect brain regions which encode differences between vocal and non-vocal stimuli. Following the MVPA workflow, the localization problem is cast as a supervised learning problem: if the type of the stimulus can be predicted from the spatial activation pattern significantly better than

chance, then a region is declared to encode vocal/non-vocal information. We call this an *accuracy test*, a.k.a. *class prediction*, or *pattern discrimination*

This same signal detection task can be also approached as a two-group multivariate test. Inferring that a region encodes vocal/non-vocal information, is essentially inferring that the spatial distribution of brain activations is different given a vocal/non-vocal stimulus. As put in Pereira et al. [2009]:

... the problem of deciding whether the classifier learned to discriminate the classes can be subsumed into the more general question as to whether there is evidence that the underlying distributions of each class are equal or not.

A practitioner may thus approach the signal detection problem with a two-group population test such as Hotelling's T^2 [Anderson, 2003]. Alternatively, if the size of brain region of interest is large compared to the number of observations, so that the spatial covariance cannot be fully estimated, then a high dimensional version of Hotelling's test can be called upon, such as in Schäfer and Strimmer [2005] or Srivastava [2007]. For brevity, and in contrast to *accuracy tests*, we will call any two-sample multivariate tests simply *population tests*, a.k.a. *class comparisons*. [TODO: rename population test to parameter test?]

At this point, it becomes unclear which is preferable: a population test or an accuracy test? The former with a heritage dating back to Hotelling [1931], and the latter being extremely popular, as the 959 citations¹ of Kriegeskorte et al. [2006] suggest.

The comparison between population and accuracy tests was precisely the goal of Ramdas et al. [2016], who compared the T^2 population test to the accuracy of *Fisher's linear discriminant analysis* classifier (LDA). By comparing the rates of convergence of the powers to 1, Ramdas et al. [2016] concluded that accuracy and population tests are rate equivalent.

Asymptotic relative efficiency measures (ARE) are typically used by statisticians to compare between rate-equivalent test statistics [van der Vaart, 1998]. Ramdas et al. [2016] derive the asymptotic power functions of the two test statistics, which allows to compute the ARE between Hotelling's T^2 (population) test and Fisher's LDA (accuracy) test. Theorem 14.7 of van der Vaart [1998] relates asymptotic power functions to ARE. Using this theorem and the results of Ramdas et al. [2016] we deduce that the ARE is lower bounded by $2\pi \approx 6.3$. This means that Fisher's LDA requires at least 6.3 more samples to achieve the same (asymptotic) power than the T^2 test. In

¹GoogleScholar. Accessed on Aug 4, 2016.

63 this light, the accuracy test is remarkably inefficient compared to the pop-
64 ulation test. For comparison, the t-test is only 1.04 more (asymptotically)
65 efficient than Wilcoxon’s rank-sum test [Lehmann, 2009], so that an ARE of
66 6.3 is strong evidence in favor of the population test.

67 Before discarding accuracy tests as inefficient, we recall that Ramdas
68 et al. [2016] analyzed a *half-sample* holdout. The authors conjectured that a
69 leave-one-out approach, which makes more efficient use of the data, may have
70 better performance. Also, the analysis in Ramdas et al. [2016] is asymptotic.
71 This eschews the discrete nature of the accuracy statistic, which will be
72 shown to have crucial impact. Since typical sample sizes in neuroscience are
73 not large, we seek to study which test is to be preferred in finite samples?
74 Our conclusion will be quite simple: *population tests typically have more*
75 *power than accuracy tests, and are easier to implement.*

76 Our statement rests upon the observation that with typical sample sizes,
77 the accuracy test statistic is highly discrete. Permutation testing with dis-
78 crete test statistics are known to be conservative [Hemerik and Goeman,
79 2014], since they are insensitive to mild perturbations of the data, and they
80 cannot exhaust the permissible false positive rate. As simply put by Frank
81 Harrell in CrossValidated² post back in 2011:

82 ... your use of proportion classified correctly as your accuracy
83 score. This is a discontinuous improper scoring rule that can be
84 easily manipulated because it is arbitrary and insensitive.

85 The degree of discretization is governed by the number of samples. In our
86 neuroscience example from Gilron et al. [2016], the classification is performed
87 based on 40 trials, so that the test statistic may assume only 40 possible
88 values. This number of examples is not unusual if considering this is the
89 number of trial-repeats, or the number of subjects, in a neuroimaging study.

90 The discretization effect is aggravated if the test statistic is highly concen-
91 trated. For an intuition consider the usage of a the *resubstitution accuracy*
92 as a test statistic. This statistic simply means that the accuracy is not cross
93 validated, but rather evaluated on the training data. If the data is high
94 dimensional, the resubstitution accuracy will be very high due to over fit-
95 ting. In a very high dimensional regime, the resubstitution accuracy will
96 be 1 for the observed data [McLachlan, 1976, Theorem 1], but also for any
97 permutation. The concentration of resubstitution accuracy near 1, and its
98 discreteness, render this test completely useless, with power tending to 0 for
99 any (fixed) effect size, as the dimension of the model grows.

²A Q&A website for statistical questions: <http://stats.stackexchange.com/questions/17408/how-to-assess-statistical-significance-of-the-accuracy-of-a-classifier>

100 To compare the power of accuracy tests and population tests in finite
 101 samples, we study a battery of test statistics by means of simulation. We start
 102 with formalizing the problem in Section 2. The main findings are reported
 103 in Sections 4, 5 and Appendix C. A discussion follows in Section 6.

104 2 Problem setup

105 Let $y \in \mathcal{Y}$ be a class encoding. Let $x \in \mathcal{X}$ be a p dimensional feature vector.
 106 In our vocal/non-vocal example we have $\mathcal{Y} = \{-1, 1\}$ and p , the number of
 107 voxels in a brain region so that $\mathcal{X} = \mathbb{R}^{27}$.

108 Given n pairs of (x_i, y_i) , typically assumed i.i.d., a population test amounts
 109 to testing whether $x|y = 1$ has the the same distribution as $x|y = -1$. I.e.,
 110 we test if the multivariate voxel activation pattern has the same distribution
 111 when given a vocal stimulus, as when given a non-vocal stimulus.

An accuracy test amounts to learning a predictive model and testing if its
 predictions $y|x$ are better than chance. Denoting a dataset by $\mathcal{S} := (x_i, y_i)_{i=1}^n$,
 the a predictor, $\mathcal{A}_{\mathcal{S}}(x) : \mathcal{X} \rightarrow \mathcal{Y}$, is the output of a learning algorithm \mathcal{A} when
 applied to the dataset \mathcal{S} , so that $\mathcal{A} : \mathcal{S} \rightarrow \mathcal{A}_{\mathcal{S}}(x)$. The accuracy of predictor,
 $\mathcal{E}_{\mathcal{A}_{\mathcal{S}}(x)}$, is defined as the probability of $\mathcal{A}_{\mathcal{S}}(x)$ making a correct prediction.
 The accuracy of an algorithm, $\mathcal{E}_{\mathcal{A}}$, is defined as the expected accuracy over
 all possible data sets. Formally—denoting by \mathcal{P} the probability measure of
 (x, y) , and by \mathcal{P}^n the same for the i.i.d sample \mathcal{S} , then

$$\mathcal{E}_{\mathcal{A}_{\mathcal{S}}(x)} := \int_{(x,y)} \mathcal{I}\{\mathcal{A}_{\mathcal{S}}(x) = y\} d\mathcal{P}(x, y), \quad (1)$$

and

$$\mathcal{E}_{\mathcal{A}} := \int_{\mathcal{S}} \mathcal{E}_{\mathcal{A}_{\mathcal{S}}} d\mathcal{P}^n(\mathcal{S}). \quad (2)$$

112 Denoting an estimate of $\mathcal{E}_{\mathcal{A}_{\mathcal{S}}(x)}$ by $\hat{\mathcal{E}}_{\mathcal{A}_{\mathcal{S}}(x)}$, and $\mathcal{E}_{\mathcal{A}}$ by $\hat{\mathcal{E}}_{\mathcal{A}}$, a statistically sig-
 113 nificant “better than chance” estimate of either, is evidence that the classes
 114 are distinct. In a typical application, the predictor is not fixed, so that $\hat{\mathcal{E}}_{\mathcal{A}}$,
 115 and not $\hat{\mathcal{E}}_{\mathcal{A}_{\mathcal{S}}(x)}$, will be used for the testing.

116 Two popular estimates of $\hat{\mathcal{E}}_{\mathcal{A}}$ are the *resubstitution estimate*, and the
 117 V-fold cross validation (CV) estimate.

Definition 1 (Resubstitution estimate). The resubstitution accuracy esti-
 mator, $\hat{\mathcal{E}}_{\mathcal{A}}^{Resub}$, is defined as

$$\hat{\mathcal{E}}_{\mathcal{A}}^{Resub} := \frac{1}{n} \sum_{i=1}^n \mathcal{I}\{\mathcal{A}_{\mathcal{S}}(x_i) = y_i\}, \quad (3)$$

118 where $\mathcal{I}\{A\}$ is the indicator function of event A .

Definition 2 (V-fold CV estimate). Denoting by \mathcal{S}^v the v 'th partition, or *fold*, of the dataset, and by $\mathcal{S}^{(v)}$ its complement, so that $\mathcal{S}^v \cup \mathcal{S}^{(v)} = \cup_{v=1}^V \mathcal{S}^v = \mathcal{S}$, the V-fold CV accuracy estimator, $\hat{\mathcal{E}}_{\mathcal{A}}^{Vfold}$, is defined as

$$\hat{\mathcal{E}}_{\mathcal{A}}^{Vfold} := \frac{1}{V} \sum_{v=1}^V \frac{1}{|\mathcal{S}^v|} \sum_{i \in \mathcal{S}^v} \mathcal{I}\{\mathcal{A}_{\mathcal{S}^{(v)}}(x_i) = y_i\}, \quad (4)$$

119 2.1 Candidate Tests

120 The design of a permutation test using $\hat{\mathcal{E}}_{\mathcal{A}}$ requires the following design
121 choices:

- 122 1. Is $\hat{\mathcal{E}}_{\mathcal{A}}$ cross validated or not?
- 123 2. For a V-fold cross validated test statistic:
 - 124 (a) Should the data be refolded in each permutation?
 - 125 (b) Should the data folding be balanced (a.k.a. stratified)?
 - 126 (c) How many folds?
- 127 3. How to estimate $\hat{\mathcal{E}}_{\mathcal{A}}$?

128 We will now address these questions while bearing in mind that unlike
129 the typical supervised learning setup, we are not interested in an unbiased
130 estimate of $\mathcal{E}_{\mathcal{A}}$, but rather in the detection of its departure from chance level.

131 **Cross validate or not?** Given our goal, a biased estimate of $\hat{\mathcal{E}}_{\mathcal{A}}$ is not a
132 problem provided that bias is consistent over all permutations. The under-
133 lying intuition is that a permutation test will be unbiased, provided that the
134 exact same computation is performed over all permutations. We will thus be
135 considering both cross validated accuracies, and resubstitution accuracies.

136 **Balanced folding?** The standard practice when cross validating is to con-
137 strain the data folds to be balanced, i.e. stratified [e.g. Ojala and Garriga,
138 2010]. This means that each fold has the same number of examples from
139 each class. We will report results with both balanced and unbalanced data
140 foldings, only to discover, it does not seem to matter.

141 **Refolding?** The standard practice in neuroimaging is to permute labels
 142 and refold the data after each permutation, so that the balance of the classes
 143 in each fold is preserved. We will adhere to this practice due to its popularity,
 144 even though it can be avoided by permuting features instead of labels, as done
 145 by Golland et al. [2005].

146 **How many folds?** Different authors suggest different rules for the number
 147 of folds. We will look into the effect of the number of folds.

How to estimate accuracy? Lower than 0.5 accuracies, known as *anti-learning*, are evidence that signal is present and classes are separated. Given out detection purposes, we should consider the departure from chance level $|\hat{\mathcal{E}}_{\mathcal{A}} - 0.5|$ as candidate test statistic. For unbalanced classes, chance level is not 0.5, but rather the probability of the majority class, which we denote by $\hat{\mathcal{E}}_{Maj}$. This suggests the following test statistic $|\hat{\mathcal{E}}_{\mathcal{A}} - \hat{\mathcal{E}}_{Maj}|$. Since we will be aggregating these statistics over random data sets where $\hat{\mathcal{E}}_{Maj}$ may vary, it seems appropriate to standardize the scale. We thus study, along with the naive accuracy estimate, $\hat{\mathcal{E}}_{\mathcal{A}}$, also the *z-scored accuracy* of algorithm \mathcal{A} :

$$\hat{\mathcal{Z}}_{\mathcal{A}} := \frac{|\hat{\mathcal{E}}_{\mathcal{A}} - \hat{\mathcal{E}}_{Maj}|}{\sqrt{\hat{\mathcal{E}}_{Maj}(1 - \hat{\mathcal{E}}_{Maj})}}. \quad (5)$$

148 Table 1 collects an initial battery of tests we will be comparing.

Name	Algorithm	Accuracy	Z-scored	Parameters
Hotelling	Hotelling	—	—	—
Hotelling.shrink	Hotelling	—	—	—
sd	Hotelling	—	—	—
lda.CV.1	LDA	V-fold	FALSE	—
lda.CV.2	LDA	V-fold	TRUE	—
lda.noCV.1	LDA	Resubstitution	FALSE	—
lda.noCV.2	LDA	Resubstitution	TRUE	—
svm.CV.1	SVM	V-fold	FALSE	cost=10
svm.CV.2	SVM	V-fold	FALSE	cost=0.1
svm.CV.3	SVM	V-fold	TRUE	cost=10
svm.CV.4	SVM	V-fold	TRUE	cost=0.1
svm.noCV.1	SVM	Resubstitution	FALSE	cost=10
svm.noCV.2	SVM	Resubstitution	FALSE	cost=0.1
svm.noCV.3	SVM	Resubstitution	TRUE	cost=10
svm.noCV.4	SVM	Resubstitution	TRUE	cost=0.1

Table 1: This table collects the various test statistics we will be studying. Three are population tests: *Hotelling*, *Hotelling.shrink*, and *sd*. *Hotelling* is the classical two-group T^2 statistic. *Hotelling.shrink* is a high dimensional version with the regularized covariance from Schäfer and Strimmer [2005]. *sd* is another high dimensional version of the T^2 , from Srivastava et al. [2013]. The rest of the tests are variations of the linear SVM, and Fisher’s LDA, with varying accuracy measures, cross validated or not, and varying tuning parameters. For example, *svm.CV.4* is a linear SVM (implemented with the *svm* R function [Meyer et al., 2015]), the cost parameter set at 0.1, and using the cross validated z-scored accuracy in Eq. 5. Another example is *lda.noCV.1*, which is Fisher’s LDA, returning the resubstitution accuracy.

149

150 3 Controlling the False Positive Rate

151 Our simulations show that all of the tests considered conserve the desired
152 0.05 false positive rate, up to varying levels of conservatism. This can be
153 seen from the fact that the probability of rejection is no larger than 0.05 in
154 the absence of any effect, encoded by a red circle. This is true, in particular
155 if:

- 156 (a) The folds are balanced or not (Figures 5,6 and 7).
- 157 (b) The tuning parameters are varied (cost=10 versus cost=0.1).
- 158 (c) The number of folds is varied (Figures 6 and 7).
- 159 (d) The noise is heavytailed (Figure 8b).

160 (e) The problem is high or low dimensional (Figure 9.)
 161 (f) The noise is correlated (Figure 10b).
 162 We also observe that the most conservative tests are the resubstitution ac-
 163 curacy statistics. We return to this matter in the Discussion.

164 4 Power

165 Having established that all of the tests in our battery control the false pos-
 166 itive rate, it remains to be seen if they have similar power— especially when
 167 comparing population tests to accuracy tests. From the simulation results
 168 reported in Appendix C we collect the following insights:

- 169 1. Population tests have no less— and typically more— power than accuracy
 170 tests in our simulations.
- 171 2. The conservativeness of accuracy tests decays as the sample grows (Fig-
 172 ures 9a, 9b and 10a)
- 173 3. For heavy tailed distributions (Figure 8b), the difference in power be-
 174 tween population tests and accuracy tests vanishes.
- 175 4. Regularization is critical to power as can be seen by comparing *Hotelling*
 176 to *Hotelling.shrink* and *sd*.
- 177 5. The z-scoring of the accuracies was introduced to deal with unbalanced
 178 foldings. If the z-scoring has any effect at all, it merely kills power. The
 179 non-z-scored accuracy tests are unaffected by the balance of the folding.
- 180 6. Both accuracy and population tests are inappropriate for scale alter-
 181 natives (Figure 8a). This was to be expected and is reported mostly as
 182 a sanity check (cost=10 vs. cost=0.1 statistics).
- 183 7. Balanced folding only affects the z-scored accuracy, in the opposite
 184 direction than we anticipated.
- 185 8. Increasing the SVM’s cost parameter, which reduces the number of
 186 support vectors entering the classifier, reduces power.

187 The major insight from simulations is that the use of accuracy tests for
 188 signal detection is underpowered compared to population tests. We have not
 189 established, however, that the dominance of the population tests is not due to
 190 their regularization. Indeed, the unregularized *Hotelling* test, is only slightly
 191 superior to the accuracy tests. We return to this matter in Section 6.4, by
 192 adding some regularized accuracy tests to our battery. We now verify our
 193 finding on a neuroimaging dataset.

194 5 Neuroimaging Example

195 Figure 1 is an application of both a population and an accuracy test to the
196 data of Pernet et al. [2015]. The authors of Pernet et al. [2015] collected fMRI
197 data while subjects were exposed to the sounds of human speech (vocal), and
198 other non-vocal sounds. Each subject was exposed to 20 sounds of each type,
199 totaling in $n = 40$ trials. The study was rather large and consisted of about
200 200 subjects. The data was kindly made available by the authors at the
201 OpenfMRI website³.

202 We perform group inference using within-subject permutations along the
203 analysis pipeline of Stelzer et al. [2013], which was also reported in Gilron
204 et al. [2016]. For completeness, the pipeline is described in Appendix A. To
205 demonstrate our point, we compare the *sd* population test with the *svm.cv.1*
206 accuracy test.

207 In agreement with our simulation results, the population test (*sd*) dis-
208 covers more brain regions of interest when compared to an accuracy test
209 (*svm.cv.1*). The former discovers 1,232 regions, while the latter only 441, as
210 depicted in Figure 1. We emphasize that both test statistics were compared
211 with the same permutation scheme, and the same error controls, so that any
212 difference in detections is due to their different power.

213 6 Discussion

214 We have set out to understand which of the tests is more powerful: accu-
215 racy tests or population tests. No amount of simulations can replace the
216 insight provided by a closed-form analytic result. The finite sample power
217 of permutation tests is a formidable mathematical problem, so we currently
218 content ourselves with simulations. We have concluded that the population
219 tests are typically preferable. Their high dimensional versions, such as Sri-
220 vastava [2007] and Schäfer and Strimmer [2005], are particularly well suited
221 for neuroimaging problems such as MVPA. We attribute this to several ef-
222 fects:

- 223 (a) The discrete nature of the accuracy test in finite samples.
- 224 (b) Inefficient use of the data when validating with a holdout set.
- 225 (c) The lack of regularization in high SNR regimes (high dimension and/or
226 strong correlations).

227
228 The degree of discretization is governed by the sample size. For this
229 reason, an asymptotic analysis such as Ramdas et al. [2016] may uncover

³<https://openfmri.org/>



Figure 1: Brain regions encoding information discriminating between vocal and non-vocal stimuli. Map reports the centers of 27-voxel sized spherical regions, as discovered by an accuracy test (*svm.cv.1*), and a population test (*sd*). *svm.cv.1* was computed using 5-fold cross validation, and a cost parameter of 1. Region-wise significance was determined using the permutation scheme of Stelzer et al. [2013], followed by region-wise $FDR \leq 0.05$ control using the Benjamini-Hochberg procedure [Benjamini and Hochberg, 1995]. Number of permutations equals 400. The population test detect 1,232 regions, and the accuracy test 441, 399 of which are common to both. For the details of the analysis see Appendix A and Gilron et al. [2016].

the holdout inefficiency, but will not uncover the discretization effect. An asymptotic analysis of a finite complexity model, such as [Golland et al., 2005, Sec 4.3], would also fail to reveal the effect of the concentration of the resubstitution accuracy near 1. This effect would render the resubstitution estimates a legitimate asymptotic test, and a terrible finite sample test.

Simulations do show cases where population tests have no advantage over accuracy tests. One such scenario is when the noise is heavytailed, as seen in Figure 8b. The second scenario will be discussed in Section 6.4.

The practical advice for the practitioner, is that for the purpose of signal detection, there is typically a population test that is more powerful than an accuracy test. The class of population tests we examined, in particular their regularized versions, are good performers in a wide range of simulation setups and empirically. They are also typically easier to implement, and faster to run, since no cross validation will be involved.

244 6.1 Ease of implementation

245 A very important consideration is the ease of implementation. The need
246 for cross validation of the accuracy test greatly increases its computational
247 complexity. Moreover, programming with discrete statistics is more prone to
248 errors. This is because their unforgiveness to the type of inequalities used.
249 Indeed, mistakenly replacing a weak inequality with a strong inequality in
250 one’s program may considerably change the results. This is not the case for
251 continuous test statistics.

252 6.2 Reservations

253 Some reservations to the generality of our findings are in order. Firstly,
254 not all accuracy tests are concerned with signal detection. Consider brain
255 decoding for machine interfaces, or clinical diagnosis, where the presence of
256 a medical condition is predicted from imaging data [e.g. Olivetti et al., 2012,
257 Wager et al., 2013]. In those examples, the purpose of the test is not to
258 detect a difference between classes, but to actually test the performance of a
259 particular classifier.

260 Secondly, it may be argued that accuracy tests permits the separation
261 between classes in high dimensions, such as in *reproducing kernel Hilbert*
262 *spaces* (RKHS) by using non-linear predictors while population tests do not.
263 This is a false argument— accuracy test do not have any more flexibility
264 that population tests. Indeed, it is possible to test for location in the same
265 space the classifier is learned. For independence tests in high dimensional
266 spaces see for example Székely and Rizzo [2009] or Gretton et al. [2012].
267 On the other hand, based on our experience, and the reported neuroimaging
268 example, we find that a population test in the original feature space is a
269 simple and powerful approach to signal detection.

270 6.3 Smoothing accuracy estimates

271 It may be possible to alleviate the effect of discretization by via the cross-
272 validation scheme. The discreteness of the accuracy statistic is governed by
273 the number of examples in the union of holdout test sets, over all retesting
274 iterations. For V-fold CV, for instance, the accuracy may assume as many
275 values as the sample size. This suggests that the accuracy can be “smoothed”
276 by allowing the test sample to be drawn with replacement. An algorithm that
277 samples test sets with replacement is the *leave-one-out bootstrap estimator*,
278 and its derivatives, such as the *0.632 bootstrap*, and *0.632+ bootstrap* [Hastie
279 et al., 2003, Sec 7.11].

Definition 3 (bLOO). The *leave-one-out bootstrap* estimate, bLOO, is the average accuracy of the holdout observations, over all bootstrap samples. Denote by \mathcal{S}^b , a bootstrap sample b of size n , sampled with replacement from \mathcal{S} . Also denote by $C^{(i)}$ the index set of bootstrap samples, b , not containing observation i . The leave-one-out bootstrap estimate, $\hat{\mathcal{E}}_{\mathcal{A}}^{bLOO}$, is defined as:

$$\hat{\mathcal{E}}_{\mathcal{A}}^{bLOO} := \frac{1}{n} \sum_{i=1}^n \frac{1}{|C^{(i)}|} \sum_{b \in C^{(i)}} \mathcal{I}\{\mathcal{A}_{\mathcal{S}^b}(x_i) = y_i\}. \quad (6)$$

where $|A|$ is the cardinality of set A . Equivalently [TODO: verify], denoting by $S^{(b)}$ the indexes of observations, i , that are *not* in the bootstrap sample b and are not empty,

$$\hat{\mathcal{E}}_{\mathcal{A}}^{bLOO} = \frac{1}{B} \sum_{b=1}^B \frac{1}{|S^{(b)}|} \sum_{i \in S^{(b)}} \mathcal{I}\{\mathcal{A}_{\mathcal{S}^b}(x_i) = y_i\}. \quad (7)$$

Definition 4 (b0.632). The *0.632 bootstrap* accuracy estimate, b0.632, is a wighted average of the resubstitution error and the bLOO. Formally:

$$\hat{\mathcal{E}}_{\mathcal{A}}^{0.632} := 0.368 \hat{\mathcal{E}}_{\mathcal{A}}^{Resub} + 0.632 \hat{\mathcal{E}}_{\mathcal{A}}^{bLOO}. \quad (8)$$

Simulation results reported in Figure 2 with naming conventions in Table 2. It can be seen that selecting test sets with replacement does increase the power, when compared to V-fold cross validation, but still falls short from the power of population tests. It can also be seen that power increases with the number of bootstrap replications, as was to be expected, since more replications reduce the level of discretization. The type of bootstrap, bLOO versus b0.632, does not change the power.

Name	Algorithm	Accuracy	B	Z-scored	Parameters
lda.Boot.1	LDA	b0.632	10	FALSE	—
lda.Boot.2	LDA	bLOO	10	FALSE	—
svm.Boot.1	SVM	b0.632	10	FALSE	cost=10
svm.Boot.2	SVM	bLOO	10	FALSE	cost=10
svm.Boot.3	SVM	b0.632	50	FALSE	cost=10
svm.Boot.4	SVM	bLOO	50	FALSE	cost=10

Table 2: The same as Table 1 for bootstrapped accuracy estimates. bLOO and b0.632 are defined in definitions 3 and 4 respectively. B denotes the number of Bootstrap samples.

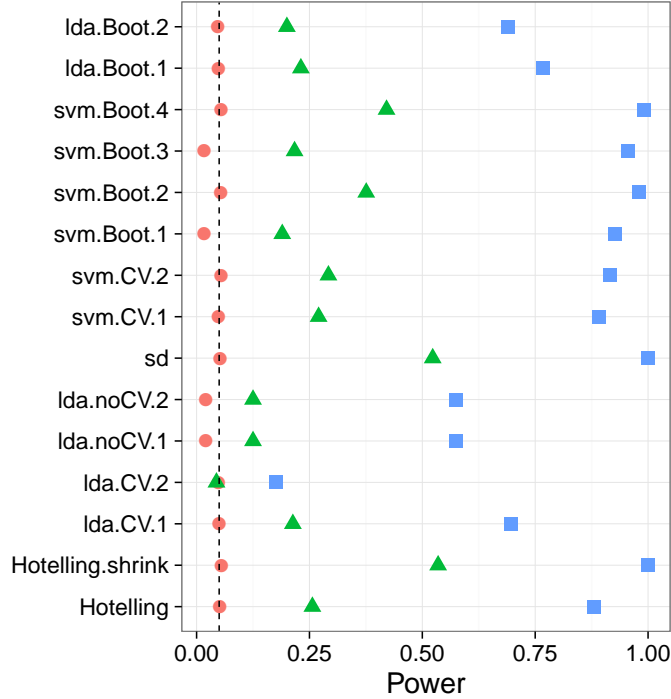


Figure 2: Bootstrap— The power of a permutation test with various test statistics. The power on the x axis. Effect are color and shape coded. The various statistics on the y axis. Their details are given in tables 1 and 2. Effects vary over 0 (red circle), 0.25 (green triangle), and 0.5 (blue square). Simulation details in Appendix B.

6.4 High dimensional classifiers

Inspecting Figure 5a (for instance), it can be seen that Hotelling’s unregularized T^2 test has similar power as accuracy tests. It should thus be argued that the real advantage of the population tests is due to their adaptation to high dimension by regularization, and not only to discretization. To study this, we call upon several *regularized classifiers*, designed for high dimensional problems. In the spirit of the regularized covariance of *Hotelling.shrink*, we try an l_2 regularized SVM [?], and shrinkage based LDA [Pang et al., 2009, Ramey et al., 2016]. In the spirit of the diagonalized covariance of *sd*, we try a diagonalized LDA [Dudoit et al., 2002], a.k.a. *Gaussian naïve Bayes*.

Simulation results reported in Figure 3 with naming conventions in Table 3. It can be seen that regularizing a classifier in high dimension, just like a parameter test, improves power. It can also be seen that (regularized) parameter tests are still more powerful than (regularized) accuracy tests. This was to be expected, since we already saw in (e.g.) Figure 5a that the unregularized parameter test, *Hotelling*, is slightly more powerful than unregularized

304 accuracy tests such as (e.g.) *svm.CV.1*.

305 We can compound the regularization with the bootstrapping from Sec-
 306 tion 6.3, to improve finite sample power of the accuracy tests. This is done in
 307 the *svm.highdim.2* and *lda.highdim.4* tests. The latter being one of the very
 308 few accuracy tests that achieve the same power as population tests. This is
 309 exciting news since it shows how to design powerful new high-powered accu-
 310 racy tests: by sampling test sets with replacement, and by regularizing the
 311 classifiers.

Name	Algorithm	Accuracy	Z-scored	Parameters
svm.highdim.1	SVM	V-fold	FALSE	cost=10, V=4
svm.highdim.2	SVM	b0.632	FALSE	cost=10, B=50
lda.highdim.1	LDA	V-fold	FALSE	V=4
lda.highdim.2	LDA	V-fold	FALSE	V=4
lda.highdim.3	LDA	V-fold	FALSE	V=4
lda.highdim.4	LDA	b0.632	FALSE	B=50

Table 3: The same as Table 1 for regularized (high dimensional) predic-
 tors. *svm.highdim.1* is an l_2 regularized SVM [Friedman et al., 2010].
svm.highdim.2 is the same with b0.632 instead of V-fold cross valida-
 tion. *lda.highdim.1* is the Diagonal Linear Discriminant Analysis of
 Dudoit et al. [2002]. *lda.highdim.2* is the High-Dimensional Regular-
 ized Discriminant Analysis of Ramey et al. [2016]. *lda.highdim.3* is the
 Shrinkage-based Diagonal Linear Discriminant Analysis of Pang et al.
 [2009]. *lda.highdim.4* is the same with b0.632.

312

313 6.5 A good accuracy test

314 For the cases a population test cannot replace an accuracy test, we collect
 315 some conclusions and best practices.

316 **Sample size.** The conservativeness of accuracy tests decrease with sample
 317 size.

318 **Regularize.** Regularization proves crucial to detection power in low signal
 319 to noise regimes: in high dimension and/or in the presence of strong correla-
 320 tions. We find that the Shrinkage-based Diagonal Linear Discriminant Anal-
 321 ysis of Pang et al. [2009] is a particularly good performer, but more research

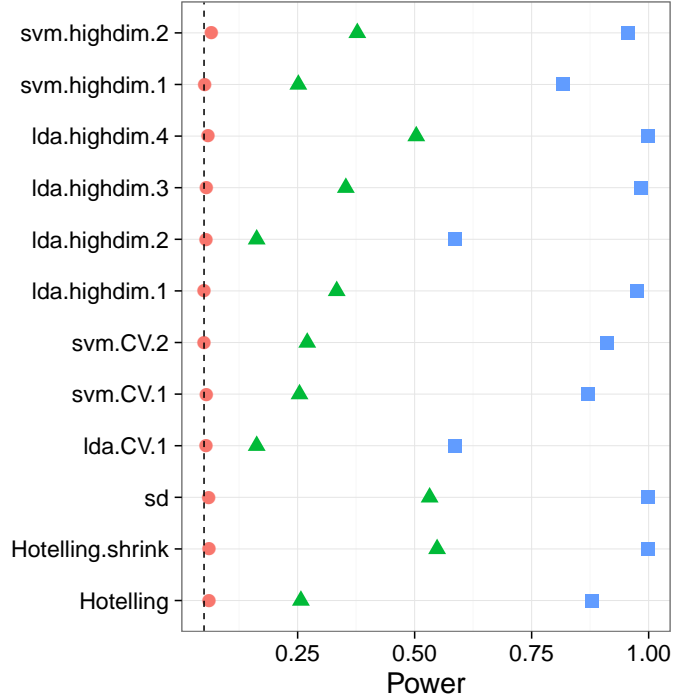


Figure 3: HighDim Classifier— The power of a permutation test with various test statistics. The power on the x axis. Effect are color and shape coded. The various statistics on the y axis. Their details are given in tables 1 and 3. Effects vary over 0 (red circle), 0.25 (green triangle), and 0.5 (blue square). Simulation details in Appendix B.

322 is required on this matter. We also conjecture that the power-maximizing
 323 regularization is larger than the error-minimizing regularization.

324 **Smooth accuracy.** Smooth accuracy estimate by cross validating with
 325 replacement. The bLOO estimator, in particular, is preferable over V-fold.

326 **Permute features.** Permuting features, such as in Golland et al. [2005], is
 327 easier than permuting labels. It allows to preserve the balance of folds after
 328 a permutation, without refolding.

329 **Resubstitution accuracy in low dimension.** Resubstitution accuracy
 330 is useful in low SNR regimes, such as low dimensional problems, because it
 331 avoids cross validation without compromising power. In high dimension, the
 332 power loss is considerable compared to a cross validated approach. We at-
 333 tribute this to the compounding of discretization and concentration effects:
 334 the difference between the sampling distribution of the resubstitution accu-

335 racy is simply indistinguishable under the null and under the alternative.
 336 In low dimensional problems, the discretization is less impactful, and the
 337 computational burden of cross validation can be avoided by using the resub-
 338 stitution accuracy. There is a fundamental difference between V-folding and
 339 resubstitution. The latter should not be thought of as the limit of the former.

340 **Don’t z-score.** There is no gain in z-scoring the accuracy scores. Our
 341 motivating rational was clearly flawed. [TODO: why?]

342 6.6 Related Literature

343 Ojala and Garriga [2010] study the power of two accuracy tests differing in
 344 the permutation scheme: One testing the “no signal” null hypothesis, and
 345 the other testing the “independent features” null hypothesis. They perform
 346 an asymptotic analysis, and a simulation study. They also apply various
 347 classifiers to various data sets. Their emphasis is the effect of the underlying
 348 classifier on the power, and the potential of the “independent features” test
 349 for feature selection. This is a very different emphasis from our own.

350 Olivetti et al. [2012] and Olivetti et al. [2014] looked into the problem
 351 of choosing a good accuracy test. They propose a new test they call an
 352 *independence test*, and demonstrate by simulation that it has more power
 353 than other accuracy tests, and can deal with non-balanced data sets. We did
 354 not include this test in the battery we compared, but we note the following:
 355 (a) The independence test of Olivetti et al. [2012] relies on a discrete test
 356 statistic. It may probably be improved with the methods discussed in this
 357 section, before the application of Olivetti et al. [2012]’s independence test.
 358 (b) In contrast with the underlying motivation of Olivetti et al. [2012]’s
 359 independence test, we did not find that balancing the data folds affects the
 360 power of the test.

361 Golland and Fischl [2003] and Golland et al. [2005] study accuracy tests
 362 using simulation, neuroimaging data, genetic data, and analytically. Their
 363 analytic results formalize our intuition from Section 1 on the effect of concen-
 364 tration of the accuracy statistic: The finite Vapnik–Chervonenkis dimension
 365 requirement [Golland et al., 2005, Sec 4.3] prevents the permutation p-value
 366 from (asymptotically) concentrating near 1. Like ourselves, they also find
 367 that the power increases with the size of the test set. This is seen in Fig.4 of
 368 Golland et al. [2005], where the size of the test-set, K , governs the discretiza-
 369 tion. Since they permute features, not labels, then all their permutation
 370 samples are balanced, and there is no issue of refolding.

Golland et al. [2005] simulate the power of accuracy tests by sampling
 from a Gaussian mixture family of models, and not from a location family

as our own simulations. Under their model

$$(x_i|y_i = 1) \sim p\mathcal{N}(\mu_1, I) + (1 - p)\mathcal{N}(\mu_2, I)$$

and

$$(x_i|y_i = -1) \sim (1 - p)\mathcal{N}(\mu_1, I) + p\mathcal{N}(\mu_2, I).$$

371 Varying p interpolates between the null distribution ($p = 0.5$) and a location
 372 shift model ($p = 0$). We now perform the same simulation as Golland et al.
 373 [2005], after parameterizing p so that $p = 0$ corresponds to the null model,
 374 and in the same dimensionality as our previous simulations We find that also
 375 in this mixture class of models a population test has more power than an
 376 accuracy test (Figure 4).

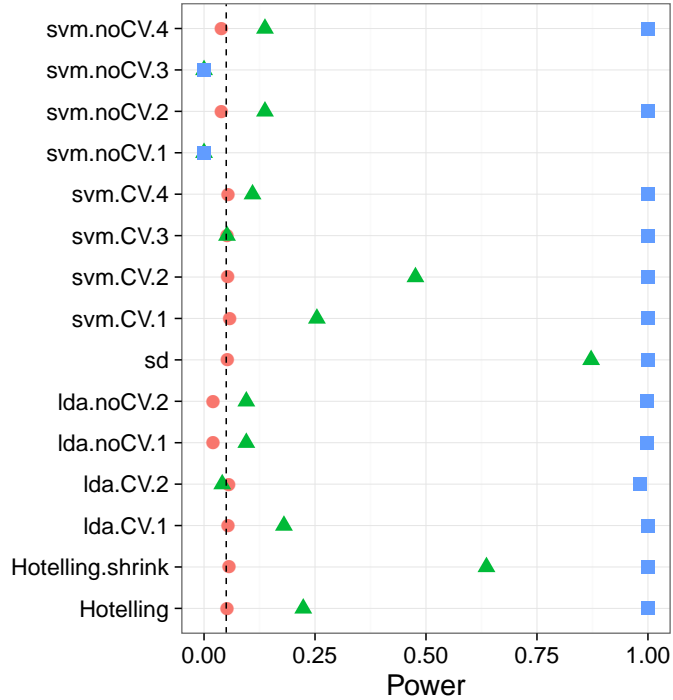


Figure 4: **Mixture**— $\mathbf{x}_i = \chi_i \mu + \eta_i$; $\chi_i = \{-1, 1\}$ and $\text{Prob}(\chi_i = 1) = (1/2 - p)^{\mathbf{y}_i^*} (1/2 + p)^{1 - \mathbf{y}_i^*}$. μ is a p -vector with $3/\sqrt{p}$ in all coordinates. The effect, p , is color and shape coded and varies over 0 (red circle), 1/4 (green triangle) and 1/2 (blue square).

377 6.7 Epilogue

378 Given all the above, we find the popularity of accuracy tests for signal de-
 379 tection quite puzzling. We believe this is due to a reversal of the inference

380 cascade. Researchers first fit a classifier, and then ask if the classes are
381 any different. Were they to start by asking if classes are any different, and
382 only then try to classify, then population tests would naturally arise as the
383 preferred method. As put by Ramdas et al. [2016]:

384 The recent popularity of machine learning has resulted in the ex-
385 tensive teaching and use of prediction in theoretical and applied
386 communities and the relative lack of awareness or popularity of
387 the topic of Neyman-Pearson style hypothesis testing in the com-
388 puter science and related “data science” communities.

389 **7 Acknowledgments**

References

- T. W. Anderson. *An Introduction to Multivariate Statistical Analysis*. Wiley-Interscience, Hoboken, NJ, 3 edition edition, July 2003. ISBN 978-0-471-36091-9.
- Y. Benjamini and Y. Hochberg. Controlling the false discovery rate: a practical and powerful approach to multiple testing. *JOURNAL-ROYAL STATISTICAL SOCIETY SERIES B*, 57:289–289, 1995.
- S. Dudoit, J. Fridlyand, and T. P. Speed. Comparison of Discrimination Methods for the Classification of Tumors Using Gene Expression Data. *Journal of the American Statistical Association*, 97(457):77–87, Mar. 2002. ISSN 0162-1459. doi: 10.1198/016214502753479248.
- J. Friedman, T. Hastie, and R. Tibshirani. Regularization Paths for Generalized Linear Models via Coordinate Descent. *Journal of Statistical Software*, 33(1):1–22, 2010.
- R. Gilron, J. Rosenblatt, O. Koyejo, R. A. Poldrack, and R. Mukamel. Quantifying spatial pattern similarity in multivariate analysis using functional anisotropy. *arXiv:1605.03482 [q-bio]*, May 2016.
- P. Golland and B. Fischl. Permutation tests for classification: towards statistical significance in image-based studies. In *IPMI*, volume 3, pages 330–341. Springer, 2003.
- P. Golland, F. Liang, S. Mukherjee, and D. Panchenko. Permutation Tests for Classification. In P. Auer and R. Meir, editors, *Learning Theory*, number 3559 in Lecture Notes in Computer Science, pages 501–515. Springer Berlin Heidelberg, June 2005. ISBN 978-3-540-26556-6 978-3-540-31892-7. doi: 10.1007/11503415_34.
- T. R. Golub, D. K. Slonim, P. Tamayo, C. Huard, M. Gaasenbeek, J. P. Mesirov, H. Coller, M. L. Loh, J. R. Downing, M. A. Caligiuri, C. D. Bloomfield, and E. S. Lander. Molecular Classification of Cancer: Class Discovery and Class Prediction by Gene Expression Monitoring. *Science*, 286(5439):531–537, Oct. 1999. ISSN 0036-8075, 1095-9203. doi: 10.1126/science.286.5439.531.
- A. Gretton, K. M. Borgwardt, M. J. Rasch, B. Schölkopf, and A. Smola. A Kernel Two-sample Test. *J. Mach. Learn. Res.*, 13:723–773, Mar. 2012. ISSN 1532-4435.

- 424 T. Hastie, R. Tibshirani, and J. Friedman. *The Elements of Statistical Learn-*
425 *ing*. Springer, July 2003. ISBN 0-387-95284-5.
- 426 J. Hemerik and J. Goeman. Exact testing with random permutations.
427 *arXiv:1411.7565 [math, stat]*, Nov. 2014.
- 428 H. Hotelling. The Generalization of Student’s Ratio. *The Annals of Math-*
429 *ematical Statistics*, 2(3):360–378, Aug. 1931. ISSN 0003-4851, 2168-8990.
430 doi: 10.1214/aoms/1177732979.
- 431 W. Jiang, S. Varma, and R. Simon. Calculating confidence intervals for
432 prediction error in microarray classification using resampling. *Statistical*
433 *Applications in Genetics and Molecular Biology*, 7(1), 2008.
- 434 L. Juan and H. Iba. Prediction of tumor outcome based on gene expression
435 data. *Wuhan University Journal of Natural Sciences*, 9(2):177–182, Mar.
436 2004. ISSN 1007-1202, 1993-4998. doi: 10.1007/BF02830598.
- 437 N. Kriegeskorte, R. Goebel, and P. Bandettini. Information-based functional
438 brain mapping. *Proceedings of the National Academy of Sciences of the*
439 *United States of America*, 103(10):3863–3868, July 2006. ISSN 0027-8424,
440 1091-6490. doi: 10.1073/pnas.0600244103.
- 441 E. L. Lehmann. Parametric versus nonparametrics: two alternative method-
442 ologies. *Journal of Nonparametric Statistics*, 21(4):397–405, 2009. ISSN
443 1048-5252. doi: 10.1080/10485250902842727.
- 444 G. J. McLachlan. The bias of the apparent error rate in discriminant analysis.
445 *Biometrika*, 63(2):239–244, Jan. 1976. ISSN 0006-3444, 1464-3510. doi:
446 10.1093/biomet/63.2.239.
- 447 D. Meyer, E. Dimitriadou, K. Hornik, A. Weingessel, and F. Leisch. *e1071:*
448 *Misc Functions of the Department of Statistics, Probability Theory Group*
449 *(Formerly: E1071), TU Wien*. 2015. R package version 1.6-7.
- 450 S. Mukherjee, P. Tamayo, S. Rogers, R. Rifkin, A. Engle, C. Campbell,
451 T. R. Golub, and J. P. Mesirov. Estimating dataset size requirements
452 for classifying DNA microarray data. *Journal of Computational Biology:*
453 *A Journal of Computational Molecular Cell Biology*, 10(2):119–142, 2003.
454 ISSN 1066-5277. doi: 10.1089/106652703321825928.
- 455 M. Ojala and G. C. Garriga. Permutation Tests for Studying Classifier Perfor-
456 mance. *Journal of Machine Learning Research*, 11(Jun):1833–1863, 2010.
457 ISSN 1533-7928.

- 458 E. Olivetti, S. Greiner, and P. Avesani. Induction in Neuroscience with
459 Classification: Issues and Solutions. In G. Langs, I. Rish, M. Grosse-
460 Wentrup, and B. Murphy, editors, *Machine Learning and Interpretation*
461 *in Neuroimaging*, number 7263 in Lecture Notes in Computer Science,
462 pages 42–50. Springer Berlin Heidelberg, 2012. ISBN 978-3-642-34712-2
463 978-3-642-34713-9. doi: 10.1007/978-3-642-34713-9_6.
- 464 E. Olivetti, S. Greiner, and P. Avesani. Statistical independence for the
465 evaluation of classifier-based diagnosis. *Brain Informatics*, 2(1):13–19, Dec.
466 2014. ISSN 2198-4018, 2198-4026. doi: 10.1007/s40708-014-0007-6.
- 467 H. Pang, T. Tong, and H. Zhao. Shrinkage-based Diagonal Discriminant
468 Analysis and Its Applications in High-Dimensional Data. *Biometrics*, 65
469 (4):1021–1029, Dec. 2009. ISSN 1541-0420. doi: 10.1111/j.1541-0420.2009.
470 01200.x.
- 471 F. Pereira, T. Mitchell, and M. Botvinick. Machine learning classifiers and
472 fMRI: A tutorial overview. *NeuroImage*, 45(1, Supplement 1):S199–S209,
473 Mar. 2009. ISSN 1053-8119. doi: 10.1016/j.neuroimage.2008.11.007.
- 474 C. R. Pernet, P. McAleer, M. Latinus, K. J. Gorgolewski, I. Charest, P. E. G.
475 Bestelmeyer, R. H. Watson, D. Fleming, F. Crabbe, M. Valdes-Sosa, and
476 P. Belin. The human voice areas: Spatial organization and inter-individual
477 variability in temporal and extra-temporal cortices. *NeuroImage*, 119:164–
478 174, Oct. 2015. ISSN 1053-8119. doi: 10.1016/j.neuroimage.2015.06.050.
- 479 M. D. Radmacher, L. M. McShane, and R. Simon. A Paradigm for
480 Class Prediction Using Gene Expression Profiles. *Journal of Computa-*
481 *tional Biology*, 9(3):505–511, June 2002. ISSN 1066-5277. doi: 10.1089/
482 106652702760138592.
- 483 A. Ramdas, A. Singh, and L. Wasserman. Classification Accuracy as a Proxy
484 for Two Sample Testing. *arXiv:1602.02210 [cs, math, stat]*, Feb. 2016.
- 485 J. A. Ramey, C. K. Stein, P. D. Young, and D. M. Young. High-Dimensional
486 Regularized Discriminant Analysis. *arXiv preprint arXiv:1602.01182*,
487 2016.
- 488 J. Schäfer and K. Strimmer. A Shrinkage Approach to Large-Scale Covariance
489 Matrix Estimation and Implications for Functional Genomics. *Statistical*
490 *Applications in Genetics and Molecular Biology*, 4(1), Jan. 2005. ISSN
491 1544-6115. doi: 10.2202/1544-6115.1175.

- 492 D. K. Slonim, P. Tamayo, J. P. Mesirov, T. R. Golub, and E. S. Lander. Class
493 Prediction and Discovery Using Gene Expression Data. In *Proceedings of*
494 *the Fourth Annual International Conference on Computational Molecular*
495 *Biology*, RECOMB '00, pages 263–272, New York, NY, USA, 2000. ACM.
496 ISBN 978-1-58113-186-4. doi: 10.1145/332306.332564.
- 497 M. S. Srivastava. Multivariate Theory for Analyzing High Dimensional Data.
498 *Journal of the Japan Statistical Society*, 37(1):53–86, 2007. doi: 10.14490/
499 jjss.37.53.
- 500 M. S. Srivastava, S. Katayama, and Y. Kano. A two sample test in high
501 dimensional data. *Journal of Multivariate Analysis*, 114:349–358, Feb.
502 2013. ISSN 0047-259X. doi: 10.1016/j.jmva.2012.08.014.
- 503 J. Stelzer, Y. Chen, and R. Turner. Statistical inference and multiple test-
504 ing correction in classification-based multi-voxel pattern analysis (MVPA):
505 Random permutations and cluster size control. *NeuroImage*, 65:69–82, Jan.
506 2013. ISSN 1053-8119. doi: 10.1016/j.neuroimage.2012.09.063.
- 507 G. J. Székely and M. L. Rizzo. Brownian distance covariance. *The Annals of*
508 *Applied Statistics*, 3(4):1236–1265, Dec. 2009. ISSN 1932-6157, 1941-7330.
509 doi: 10.1214/09-AOAS312.
- 510 A. W. van der Vaart. *Asymptotic Statistics*. Cambridge University Press,
511 Cambridge, UK ; New York, NY, USA, Oct. 1998. ISBN 978-0-521-49603-
512 2.
- 513 G. Varoquaux, P. R. Raamana, D. Engemann, A. Hoyos-Idrobo, Y. Schwartz,
514 and B. Thirion. Assessing and tuning brain decoders: cross-validation,
515 caveats, and guidelines. working paper or preprint, June 2016.
- 516 T. D. Wager, L. Y. Atlas, M. A. Lindquist, M. Roy, C.-W. Woo, and E. Kross.
517 An fMRI-Based Neurologic Signature of Physical Pain. *New England Jour-*
518 *nal of Medicine*, 368(15):1388–1397, Apr. 2013. ISSN 0028-4793. doi:
519 10.1056/NEJMoa1204471.

520 A Analysis pipeline

521 Here is the analysis pipeline of Stelzer et al. [2013] we for the auditory data in
 522 Gilron et al. [2016]. Denoting by $i = 1, \dots, I$ the subject index, $v = 1, \dots, V$
 523 the voxel index, and $s = 1, \dots, S$ the permutation index. Since regions⁴ are
 524 centered around a unique voxel, the voxel index v also serves as a unique
 525 region index. Algorithm 1 computes a region-wise test statistic, which is
 526 compared to its permutation null distribution computed by Algorithm 2.

Algorithm 1: Compute a group parametric map.

Data: fMRI scans, and experimental design.
Result: Brain map of group statistics: $\{\bar{T}_v\}_{v=1}^V$

```

1 for  $v \in 1, \dots, V$  do
2   for  $i \in 1, \dots, I$  do
3      $T_{i,v} \leftarrow$  test statistic for subject  $i$  in a region centered at  $v$ .
4    $\bar{T}_v \leftarrow \frac{1}{I} \sum_{i=1}^I T_{i,v}$ .
```

Algorithm 2: Compute a permutation p-value map.

Data: fMRI scans of 20 subjects, experimental design.
Result: Brain map of permutation p-values: $\{p_v\}_{v=1}^V$

```

1 for  $s \in 1, \dots, S$  do
2   permute labels;
3    $\bar{T}_v^s \leftarrow$  parametric map
```

⁴*searchlight* or *sphere* in the MVPA parlance

529 B Simulation Details

530 The following details are common to all the reported simulations, unless
531 stated otherwise in a figure’s caption. The R code for the simulations can be
532 found in [TODO].

533 Each simulation is based on 4,000 replications. In each replication, we
534 generate n i.i.d. samples from a shift model $\mathbf{x}_i = \mu \mathbf{y}_i^* + \eta_i$. Where $y_i^* = \{0, 1\}$
535 is the class of subject i in dummy coding. Recalling that $y_i = \{-1, 1\}$ is the
536 class in effect coding, then clearly $y_i = 2y_i^* - 1$. The noise is distributed as
537 $\eta_i \sim \mathcal{N}_p(0, \Sigma)$. The sample size $n = 40$. The dimension of the data is $p = 23$.
538 The covariance $\Sigma = I$. Effects, i.e. shifts μ , are equal coordinate p -vectors
539 with coordinates that vary over $\mu \in \{0, 1/4, 1/2\}$.

540 Having generated the data, we compute each of the test statistics in Ta-
541 ble 1. For test statistics that require data folding, we used 8 folds. We then
542 compute a permutation p-value by permuting the class labels, and recomput-
543 ing each test statistic. We perform 400 such permutations. We then reject
544 the $\mu_i = 0$ null hypothesis if the permutation p-value is smaller than 0.05.
545 The reported power is the proportion of replication where the permutation
546 p-value falls below 0.05.

C Simulation Results

Figure 5: The power of a permutation test with various test statistics. The power on the x axis. Effect are color and shape coded. The various statistics on the y axis. Their details are given in Table 1. Effects vary over 0 (red circle), 0.25 (green triangle), and 0.5 (blue square). Simulation details in Appendix B. Cross-validation was performed with balanced and unbalanced data folding. See sub-captions.

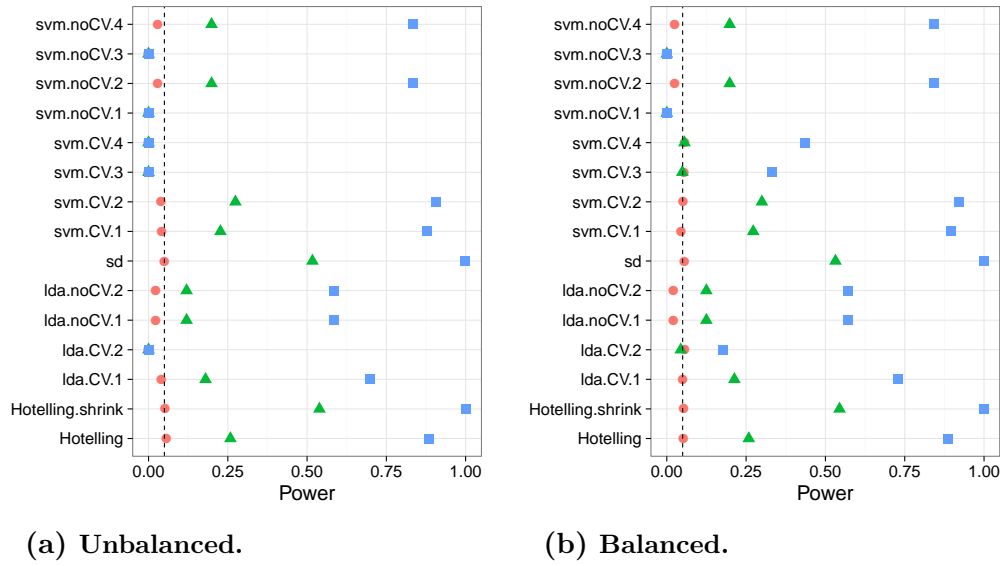


Figure 6: Simulation details in Appendix B except the changes in the sub-captions.

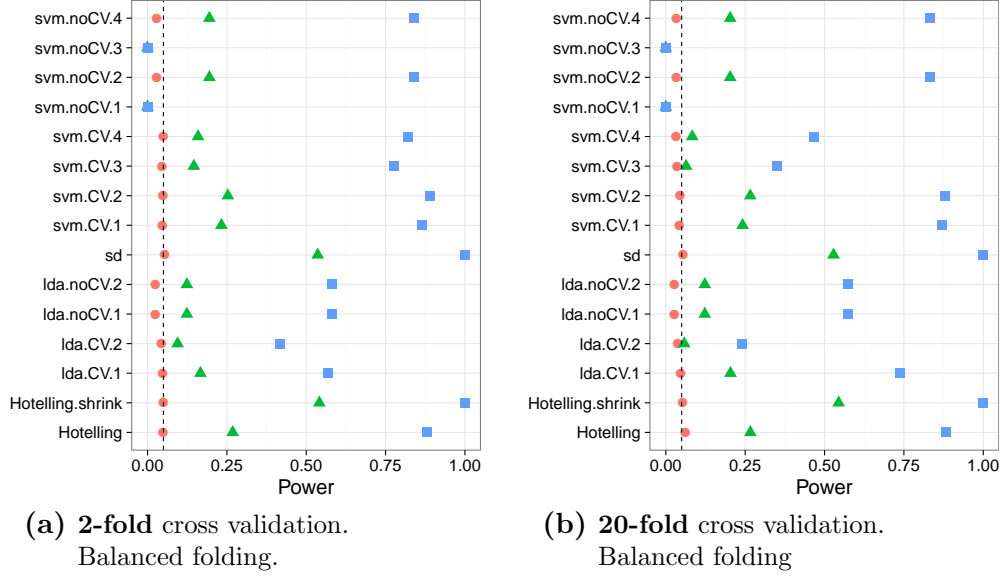


Figure 7: Simulation details in Appendix B except the changes in the sub-captions.

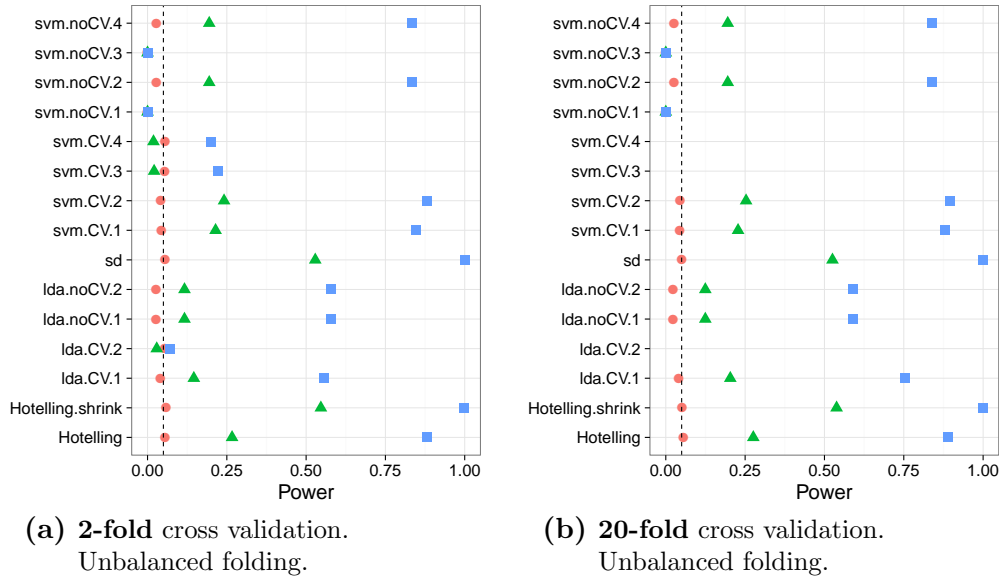


Figure 8: Simulation details in Appendix B except the changes in the sub-captions.

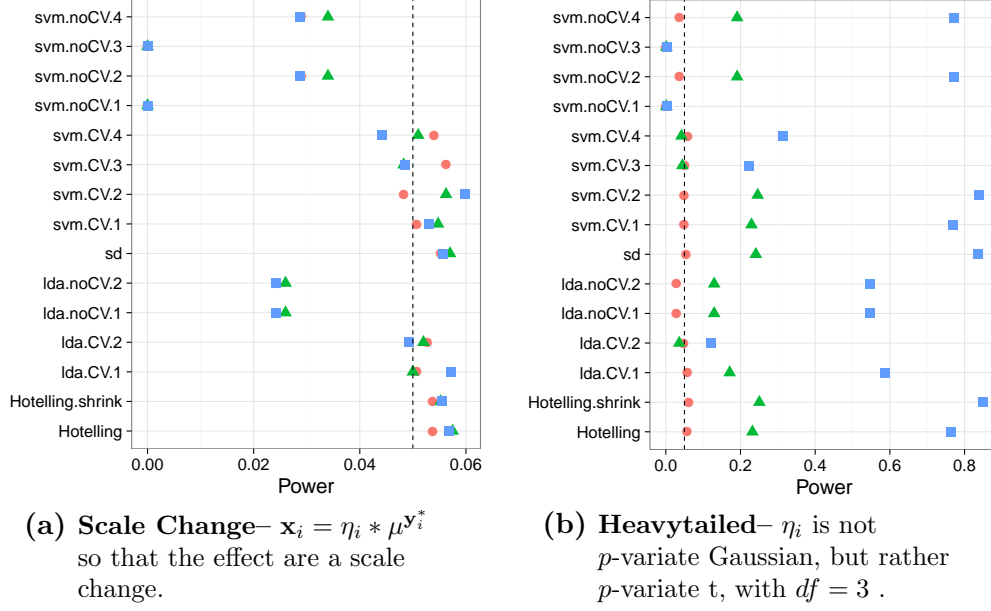


Figure 9: Simulation details in Appendix B except the changes in the sub-captions.

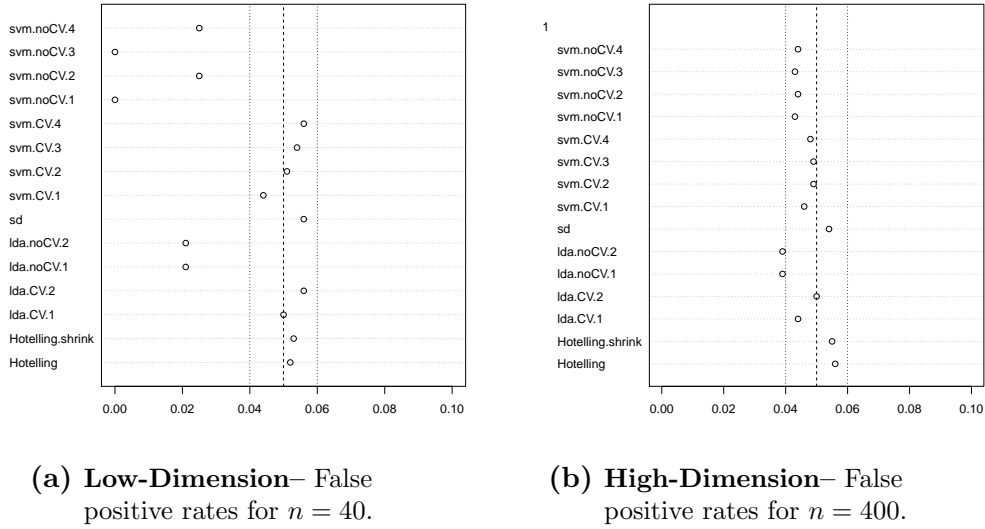
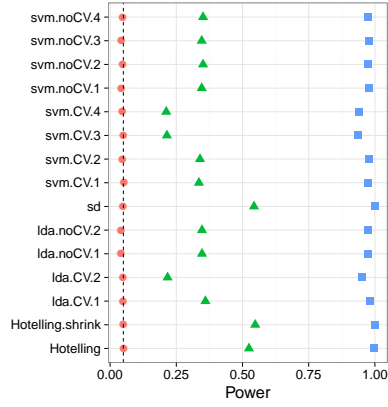
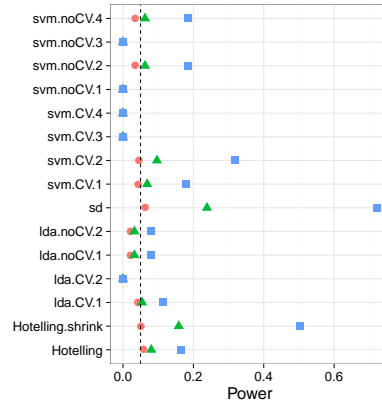


Figure 10: Simulation details in Appendix B except the changes in the sub-captions.



(a) **High-Dimension,
local alternative—**
 $n = 400,$
 $\mu \in \frac{1}{\sqrt{10}} \times \{0, 1/4, 1/2\}.$



(b) **AR(1) dependence—**
 $\Sigma_{k,l} = \rho^{|k-l|}; \rho = 0.8.$